Research Article | **Open Access**

Simulation of Frontal Protein Affinity Chromatography Using MATLAB

Patricia Guerrero-German[1]*, Rosa Ma. Montesinos-Cisneros[2] and Armando Tejeda-Mansir[3]

[1]Department of Chemical Engineering and Metallurgy, University of Sonora, L. Blvd Encinas and Rosales, Hermosillo, Sonora, Mexico
[2]Department of Mathematics, University of Sonora, L. Blvd Encinas and Rosales, Hermosillo, Sonora, Mexico
[3]Department of Scientific and Technological Research, University of Sonora, Luis Encinas and Rosales Blvd, Hermosillo, Sonora, Mexico

Abstract

In this study a transport model that includes axial dispersion in the bulk liquid, pore diffusion, external film resistance and finite kinetic rate, was used to mathematically describe a frontal affinity chromatography system. The corresponding differential equations system was solved in a simple and accurate form by using the numerical method of lines implemented in MATLAB. The solution was compared with experimental data from literature and the analytic Thomas solution. The frontal affinity chromatography of lysozyme to Cibacron Blue Sepharose was used as a model system. A good fit to the experimental data was obtained with the simulated runs of the transport model using this methodology. This approach was used to perform a parametric analysis of the experimental frontal affinity system. The solution of the transport model results in simple way to predict frontal affinity performance as well a better understanding of the fundamental mechanisms responsible for the separation.

Keywords: Mathematical modeling; Simulation; Method of lines; Affinity chromatography; Frontal analysis

Nomenclature

a   specific area/volume of the adsorbent particle (m^{-1})

c_0 initial protein concentration (mol/m^3)

c   protein concentration in the bulk liquid(mol/m^3)

c_i protein concentration in the fluid of the pores(mol/m^3)

C_D column diameter (m)

d_p adsorbent particle diameter (m)

D_{AB} protein diffusivity in free liquid (m^2/s)

D_E = $\varepsilon i D i$effective intraparticle protein diffusivity (m^2/s)

D_i intraparticle protein diffusivity (free molecular diffusivity/pore tortuosity) (m^2/s)

D_L column axial dispersion coefficient of the protein (m^2/s)

F   flow-rate (m^3/s)

k_1 adsorption rate constant ($m^3/(mol\ s)$)

k_2 desorption rate constant (s^{-1})

k_f external film mass transfer coefficient (m/s)

K_d equilibrium desorption constant, k_2/k_1

L   column length (m)

nZ   Node number in the axial direction

nR   Node number in the radial direction

P   protein molecule

PS   protein-active site complex

q_i protein concentration in the adsorbed phase of the adsorbent particles (mol/m^3)

q_m maximum equilibrium concentration,($mol/m3$) of solid volume of adsorbent

q_{ms} maximum equilibrium concentration, ($mol/m3$) of settled volume of adsorbent

r   radial distance in the adsorbent particle (m)

r_m radius of adsorbent particle (m)

S   active site

t   time (s)

v   interstitial column velocity (flow-rate/bed porosity-column area) (m/s)

z   axial distance in the column (m)

Greek Letters

ε bed porosity

ε_i adsorbent particle porosity

μ solution viscosity (g/m s)

ρ solution density (g/m^3)

Introduction

High purity products are often required from the biotechnology industry; in order to achieve the demanded purity, several complex purification steps are needed. Chromatography is used both in analytical and preparative applications in pharmaceutical and biotechnology industry [1]. Among them, affinity chromatography is the preferred choice for the primary capture step. This purification method is based on the specific interaction between the biomolecule of interest and a ligand immobilized on a solid support [2].

A preparative chromatography process is often performed in packed bed columns. The packing material is a porous gel, i.e. small beads created by a matrix of a polymer structure. There are other kinds of column configurations, like expanded beds and moving beds, but this work is focused on the traditional packed bed column.

Frontal chromatography is a widely used process in the purification

---

of biopharmaceuticals. Simulations of chromatographic processes are useful for studying and understanding complex column dynamics. When new chromatographic purification steps are planned or when an existing step is scaled up, it is common practice to perform numerous tedious chromatographic optimization experiments. As the target product molecules often are valuable and available only in small quantities, these experiments will be expensive to perform. Predicting the performance of the process by mathematical modeling and computer simulation minimizes the amount of experiments required. For this reason, simulation of chromatographic processes is becoming a valuable tool [3].

The scale-up and optimization of affinity chromatographic operations is of major industrial importance [4,5]. The development of mathematical models to describe affinity chromatographic processes, and the use of these models in computer programs to predict column performance is an engineering approach that can help to successfully attain these bioprocess engineering tasks [6]. An important requirement of this methodology is a thorough understanding of the fundamental mechanisms underlying such separations in order to develop realistic models based on basic physical and chemical principles or rate theories. The modeling in these areas often leads to a partial differential equation (PDE), or transport equation, which is parabolic in nature. Such equations may be linear, in which case analytic solutions are often achievable. However, many of the transport equations are non-linear and numerical simulations are used to understand the particular problem more fully [7].

Analytical solutions have been obtained through the rate limited breakthrough approach which considered that only one rate limiting step, i.e. either rate of interaction or rate of diffusion (pore or film) is controlling the overall adsorption mechanism. The non-dispersive flow model is used in the analysis. Chase [8] used the Thomas solution [9], which involves Langmuir reaction kinetics as the rate-limiting step, to predict the performance of affinity separations. More detailed solutions of affinity chromatography column behavior have been reported [10-14]. However, most of these methods are impracticable for the solution of transport models that include dispersed flow and finite reaction rates [5].

One of the most popular methods for solving evolutionary PDEs is the method of lines (MOL), for which efficient and effective integrating packages have been developed [15,16]. The MATLAB package has a set of strong ODE solvers, and an extensive functionality which can be used to implement the MOL [17].

The purpose of this work was to develop an accurate and simple solution of the transport model for an affinity column, using the method of lines and the MATLAB platform. The solution was compared with experimental data from the literature of the adsorption of lysozyme to Cibacron Blue Sepharose CL-6B and the Thomas analytic solution of the lumped parameter column model.

Frontal affinity chromatography model

During column operation in frontal mode the sample is fed continuously into the column. For a short time the solute in the feed is taken up almost completely, but after a while, solute breakthrough occurs and the effluent concentration increases with time. Much of the information needed to evaluate column performance is contained in these typical plots of effluent concentration versus time or breakthrough curves (BTC). These curves can be used to determine: (1) how much of the column capacity has been utilized, (2) how much solute is lost in the effluent, and (3) the processing time. This is precisely the performance information needed to optimize separation processing [18].

Many frontal affinity chromatography systems of industrial interest involve single-component adsorption. For this reason, in this study the frontal affinity model is based on the isothermal sorption of a single solute during flow through a porous fixed-bed of diffusive adsorbent particles with an average radius, r_m, and a porosity, ε_i, on which the ligand is immobilized. In this analysis, the feed protein concentration is, c_0, the protein solution in the system has a transient concentration, $c(z, t)$, with a constant interstitial flow-velocity, v, through the column, with height, L, and a void-bed porosity, ε. The protein concentrations in the adsorbent fluid and solid phases are c_i and q_i, respectively (Figure 1). To achieve a mathematical description of a frontal affinity chromatographic process, two major phenomena must be included: matrix hydrodynamics must be assessed, as well as the nature of the binding process itself. In this study, a transport model that considers a dispersed flow in the column and three consecutive transport rate resistances to ideal equilibrium separation is used for the simulation of the frontal affinity chromatography system [5].

The Fickian convective dispersion in the column is characterized by the axial dispersion coefficient, D_L. The transport of protein is considered to involve the interfacial transport of protein to the outer surface of the adsorbent particles from the bulk liquid through the adsorbent surrounding stagnant film characterized by the coefficient, k_F, the diffusion in the pore fluid described by an effective diffusion coefficient, D_E, and the adsorption step of the protein with active sites on the surface of the adsorbent. The intrinsic adsorption rate can be described by different kinetic models. In this study, an adsorption-desorption model of the Langmuir type is used.

Due to the nonlinear equilibrium that characterizes affinity chromatography, adsorption behavior is best described by rate theories. This engineering approach to modeling involves the use of conservation equations, equilibrium lawsat interfaces, kinetic laws of transport and adsorption and initial and boundary conditions. To describe the concentration change of protein with time at the column exit, the following equation can be derived by a solute mass balance in the fluid phase:
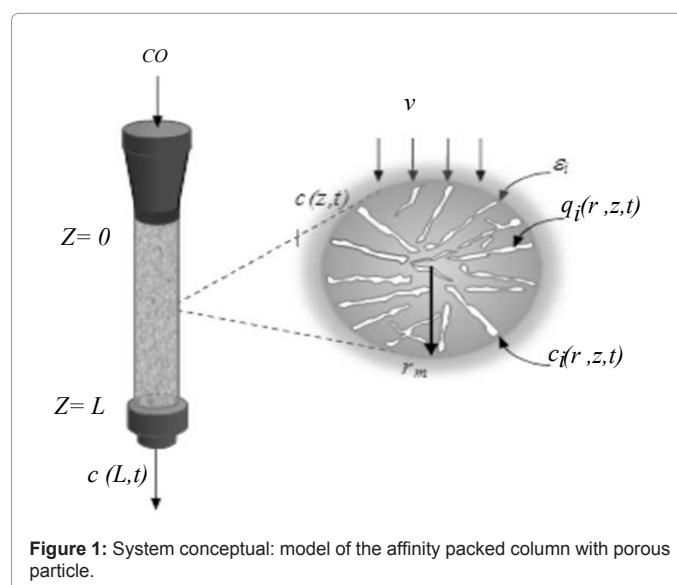

Figure 1: System conceptual: model of the affinity packed column with porous particle.

$$\frac{\partial c}{\partial t} - D_L \frac{\partial^2 c}{\partial z^2} + \upsilon \frac{\partial c}{\partial z} = -\frac{3}{r_m} \frac{(1-\varepsilon)}{\varepsilon} k_f \left(c - c_i\right)\Big|_{r=r_m} \qquad (1)$$

The equation to describe the change of concentration of solute in the fluid of the adsorbent pores can be obtained by a solute mass balance in the particle,

$$\varepsilon_i \frac{\partial c_i}{\partial t} + \left(1 - \varepsilon_i\right) \frac{\partial q_i}{\partial t} = D_E \left(\frac{\partial^2 c_i}{\partial r^2} - \frac{2}{r} \frac{\partial c_i}{\partial r}\right) \qquad (2)$$

To describe the complex interactions between solute and affinity adsorbent, simplified models are often used [8,10,18]. In general, a second-order reversible adsorption reaction is considered, where the solute is assumed to interact with the adsorbent by a monovalent interaction and characteristic constant binding energy:

$$P + S \rightarrow PS$$
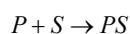
Where P is the protein in solution, S is the ligand adsorption site and PS is the protein-ligand complex.

The rate of adsorption for this type of interaction is usually represented as

$$\frac{\partial q_i}{\partial t} = k_1 c_i \left(q_m - q_i\right) - k_2 q_i \qquad (3)$$

Where k_1 and k_2 are the adsorption and desorption rate constant, respectively. At equilibrium Eq. (3) gives the form of the Langmuir isotherm with equilibrium desorption constant $K_d = k_2/k_1$ and maximum adsorption capacity q_m.

Equation (1) requires one initial condition (IC) in t (since it first order in t), two boundary conditions (BCs) in z (since it second order in r). Equation (2) also requires two IC in t (one for c_i and one for q_i) and two BCs in r.

At the beginning of the operation there is no protein present in the system, therefore ICs:

at $t = 0$,	$c = 0$	$0 \leq z \leq L$	(4)
at $t = 0$,	$c_i = 0$	$0 \leq r \leq r_m$	(5)
at $t = 0$,	$q_i = 0$	$0 \leq r \leq r_m$	(6)

The Danckwerts boundary conditions [19] are used to account for dispersion at the entrance of the column and complete mixing with only convection flow at the end of the column and given by, respectively

$$\text{at } z = 0, \qquad \varepsilon \upsilon c - \varepsilon D_L \frac{\partial c}{\partial z}\Big|_{z=0} = \varepsilon \upsilon c_0 \qquad t > 0 \qquad (7)$$

$$\text{at } z = L, \qquad \frac{\partial c}{\partial z}\Big|_{z=L} = 0 \qquad t > 0 \qquad (8)$$

Due to particle symmetry,

$$\text{at } r = 0, \qquad \frac{\partial c_i}{\partial r}\Big|_{r=0} = 0 \qquad t > 0 \qquad (9)$$

At the mouth of the particle pore,

$$\text{at } r = r_m, \qquad k_f \left(c - c_i\right)\Big|_{r=r_m} = D_E \frac{\partial c_i}{\partial r}\Big|_{r=r_m} \qquad t > 0 \qquad (10)$$

The solution to Eqs. (1)-(10) gives c(z,t), c_i(r,z,t) and q_i(r,z,t) as a function of the independent variables r,z,t.

Numerical solution of the transport model

The detailed model (Eqs. 1-10), which is based on a set of partial differential equations (PDEs), was solved numerically using the method of lines (MOL). This means that the PDEs were discretized in space, resulting in a large set of ordinary differential equations (ODEs). The set of ODEs was solved using the MATLAB ODE solver, *ode15s*, which is a variable order (1-5) and variable step-length procedure that use implicit numerical differentiation formulas (NDF) and computes the solution over each time interval [17,20].

The Figure 2 shows the numerical solution procedure. Ads_Part was used as main program. System parameters, spatial domain in radial and axial direction, the MATLAB stiff integrator ode15s and the print instructions were incorporated in Ads_Part. For the integration of ODES, parameters AbsTol = 10^{-8} and RelTol = 10^{-5} were used. The program Ads_Part_ODE calls the routines dss004 and dss044 to obtain the first and second order spatial derivatives in the axial and radial direction, using five-point, fourth-order finite difference approximations [15,21].

Since the spatial differentiation dss routines compute numerical derivatives of one dimension (1D) array (vector), a conversion from two dimensions (2D) to 1D is first required at each value of z, to compute the change of concentration of solute in the fluid of the adsorbent pores. Then the first-order radial derivatives can be computed by call to dss004. Likewise, the second derivatives in r can be computed by called to dss044 [16]. nZ discretization points were used in the column axial domain and nR discretization points were used in the particle radius. A grid analysis was used to compare the breakthrough curve sharpness using a different number of discretization points. A significant decrease in curve dispersion was observed with an increase in the number of discretization points. The total number of grid points was nZxnR. Since Eq. (2) and Eq. (3) are function of the independent variables (r,z,t) and Eq. (1) is a function of the independent variables (z,t) there were (2×nZ×nR+nZ)ODEs programmed in the ODE routine.

The initial conditions, Eq. (4) is one of single dimension vector c(z)=0, the Eqs (5, 6) are two dimension vector c_i(r,z)=0 and q_i(r,z)=0 which are converted to initial conditions single dimension vector, (y_0) with (2×nZ×nR+nZ) rows. All the codes were incorporated in a MATLAB program that was run in a personal computer. The computational times to obtain a complete breakthrough curve vary between 0.8 min and 3 min.
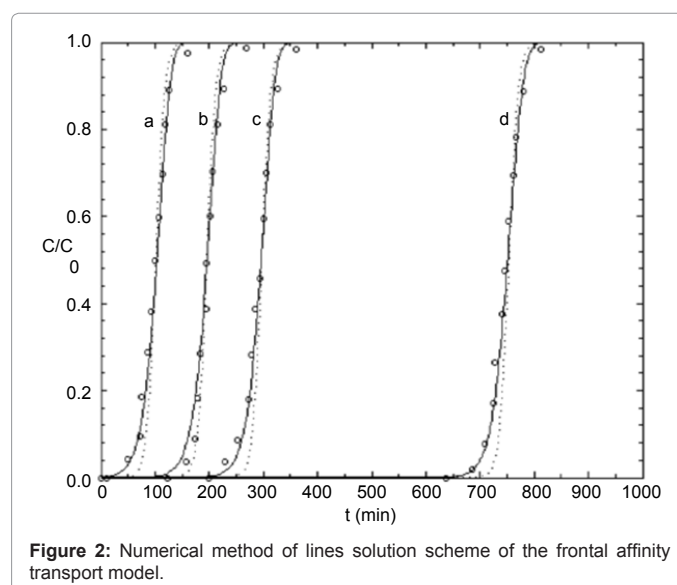

Figure 2: Numerical method of lines solution scheme of the frontal affinity transport model.

Lumped parameter model

The most general relation that has been developed to describe break through behavior involves Langmuir reaction kinetics as the rate-limiting step and non-dispersive convective flow through the column. It is known as the Thomas model [9]. Without mass-transfer effects on column performance, the overall rate of adsorption is only limited by the intrinsic adsorption kinetics. Another interpretation is that under mass-transfer limitations all effects of internal and external diffusion within and outside the beads as well as any dispersion in the column are lumped together with the kinetics. This approach is useful when mass-transfer resistance by pore-diffusion is relatively small. In this particular case, the analytical solution of the non-dispersive model is expressed as follows:

$$X = \frac{J(N/\Upsilon, N\Gamma)}{J(N/\Upsilon, N\Gamma) + \left[1 - J(N, N\Gamma/\Upsilon)\right] \exp\left[(1 - 1/\Upsilon)(N - N\Gamma)\right]} \quad (11)$$

Where

$$X = \frac{c}{c_0} \quad (12)$$

$$\Gamma = \frac{\varepsilon K_d \Upsilon (T - 1)}{(1 - \varepsilon) q_m} \quad (13)$$

$$\Upsilon = 1 + \frac{c_0}{K_d} \quad (14)$$

$$T = \frac{\upsilon t}{L} \quad (15)$$

$$N = \frac{(1 - \varepsilon) q_m k_1 L}{\varepsilon \upsilon} \quad (16)$$

and J is a two-parameter function of α and β, given by:

$$J(\alpha, \beta) = 1 - e^{-\beta} \int_0^\alpha e^{-\xi} I_0 \left(2\sqrt{\beta \xi}\right) d\xi \quad (17)$$

Where I_0 refers to the zero-order modified Bessel function of the first kind [22]. The analytical solution of Eqs. (11-17) (or Thomas model) was evaluated numerically for comparison with the numerical MATLAB solution and experimental data.

Input data for the study

The adsorption of lysozyme to Cibacron Blue Sepharose CL-6B was chosen as the model system. The values of the parameters utilized to conduct the simulation studies were obtained from the studies of [5,8,13] are presented in Table 1. To properly conduct this simulation, the experimental data were displaced one column residence time; because the time t in Chase's paper [8] is measured from the time at which non-adsorbing species exit the column. In this work, t is measured starting from the time at which the feed is introduced to the front of the bed. This last definition is commonly used in chromatography analysis because this time measurement is independent of the size of the non-adsorbing species, which is less ambiguous. The maximum adsorption capacity was calculated with respect to bed porosity, ε, and available volume to the protein as $q_m = 0.8 \times q_{ms}/[(1 - \varepsilon)(1 - \varepsilon_i)]$. In the analysis of the influence of bead diameter on the affinity process the mass-transfer coefficient was estimated using the Foo and Rice correlation [23].

$$Sh = 2 + 1.45 Re_p^{1/2} Sc^{1/3} \quad (18)$$

Where,

$$Sh = \frac{k_f d_p}{D_{AB}}, \qquad Sc = \frac{\mu}{\rho D_{AB}}, \qquad Re_p = \frac{d_p (\varepsilon \upsilon) \rho}{\mu} \quad (19)$$

Results and Discussion

The solution to the transport model for frontal affinity chromatography of lysozyme to Cibacron Blue Sepharose CL-6B was obtained using the MOL and MATLAB. This solution was compared with the experimental data and with the analytical solution of the lumped parameter model. Four column lengths were considered: 0.014, 0.027, 0.041 and 0.104 m.

The grid studied performed showed that in order to minimize the numeric dispersion, the number of nodes in the axial direction, nZ, was set to 40, 60, 80 and 100 for the 0.014, 0.027, 0.041 y 0.104 m column length simulations, respectively. The number of nodes in the radial direction was kept constant, nR=8, for all column lengths, since equal results were obtained with greater values of this parameter, an expenses of more computing time.

The results of the simulation of the breakthrough curve for the affinity column are shown in Figure 3. Taking into account the four column lengths, the average of the residual sum of squares between model calculations and experimental data were 0.0167 ± 0.0058 and 0.1146 ± 0.0776 for the MATLAB and the Thomas solution, respectively. A much better fit to the experimental data was obtained using MATLAB solution. In these computations, the kinetic parameter value was set to k1=1.144 m³/(mol s), since in the transport model this is not a lumped parameter. The simulation runs with the Thomas model using the value for the lumped parameter k_1=0.286 m³/(mol s) fitted fairly well to the experimental data.

Simulation studies

The MATLAB solution of the transport model was used to carry out a parametric analysis comparing frontal affinity curves from several computer simulations, in which one parameter was changed while the others were kept constant at the basic set of values in Table 1 and using a column length of L=0.014 m. Furthermore to describe in more detailed form the affinity chromatography process, e.g. detailing the protein dimensionless concentration profiles in the adsorbent pore
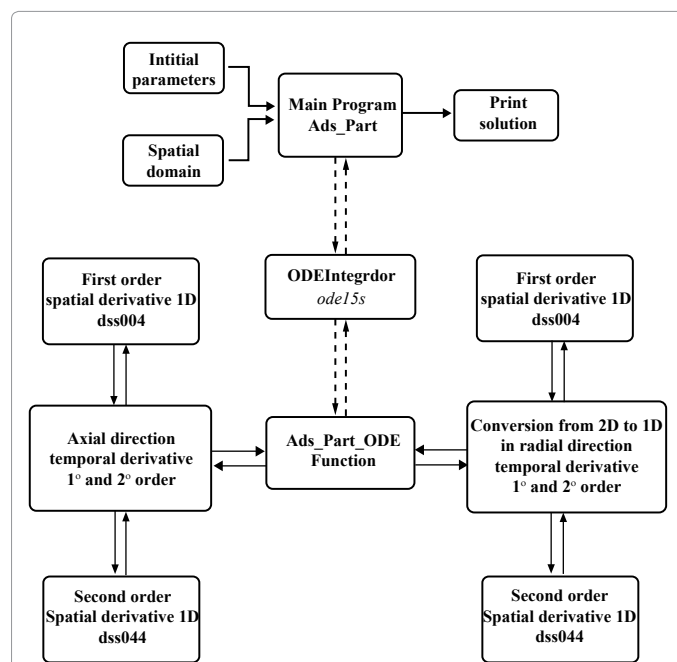

Figure 3: Transport and lumped kinetic parameter models compared with frontal affinity chromatography experimental data [8]. Operating conditions according to Table 1. (o) Experimental data. (—) Numerical method of lines solution of the transport model. (…) Lumped parameter model. The column lengths used were (a) 0.014m (b) 0.027 m, (c) 0.041m and (d) 0.104 m.

Variable	Value
Inlet protein concentration	$c_0 = 7.14 \times 10^{-3}$ mol/m³
Flow-rate	$F = 1.67 \times 10^{-8}$ m³/s
Column length	$L = 0.014, 0.027, 0.041, 0.104$ m
Column diameter	$C_D = 0.01$ m
Bed porosity	$\varepsilon = 0.39$
Bead porosity	$\varepsilon_t = 0.75$
Bead radius	$r_m = 5 \times 10^{-5}$ m
Axial dispersion	$D_L = 5.75 \times 10^{-8}$ m2/s
Film mass-transfer rate	$k_f = 6.9 \times 10^{-6}$ m/s
Solution viscosity	$\mu = 0.95$ g/m.s
Solution density	$\rho = 1.0 \times 10^{6}$ g/m³
Lysozyme diffusivity in free liquid	$D_{AB} = 1.06 \times 10^{-10}$ m²/s
Effective diffusion coefficient	$D_E = 5.3 \times 10^{-11}$ m²/s
Adsorption rate constant (Transport model)	$k_1 = 1.144$ m³/(mol s)
Adsorption rate constant (Thomas model)	$k_1 = 0.286$ m³/(mol s)
Equilibrium desorption constant	$K_d = 1.748 \times 10^{-3}$ mol/m³
Maximum adsorption capacity	$q_{ms} = 1.0$ mol/m³
Maximum adsorption capacity of solid gel	$q_m = 5.246$ mol/m³

Table 1: Base case data used in simulation studies of frontal affinity adsorption of lysozyme to Cibacron Blue Sepharose CL-6B [5,8,13].

liquid (average), c_{iAV}/c_0 and in the adsorbed phase (average), q_{iAV}/q_m as function of the dimensionless column length, Z, and the real time, t. The effect of inlet protein concentration and bead diameter is reported.

Upstream perturbations can initiate changes in process inlet concentrations that are important for study. The inlet protein concentration was changed using ± 40% variations of the $c_0 = 7.14 \times 10^{-3}$ mol/m³ base value. The corresponding curves are shown in Figure 4.

An increased inlet concentration gives an early and sharper break through curve (Figure 4). The concentration profiles are very symmetric suggesting the importance of both liquid film and pore diffusion mass transfer resistances in the adsorption process. The total column equilibration occurs in about 250, 150 and 120 min, respectively. The slope of the curves in the 0.5 region indicates the additional contribution of the dispersion to curve spreading.

As the inlet concentration increases, the driving-force for the transport process is also augmented. This results in a faster equilibration of the adsorbent beads. When the beads became equilibrated more rapidly, they will extract protein from the mobile phase for a shorter time, resulting in a sharper breakthrough curve. Hence, on this basis, it is more efficient to apply solute at high concentration. The utilization of the maximum capacity of the bed is greater at higher solute concentration as these conditions favor a greater extent of adsorption at equilibrium. As reported by Chase [8], when the dimensionless exit concentration of the column is plotted against the adsorbent applied to the column, an effect is only noticed on the shape and position of the breakthrough curve when the inlet concentration, c0, is comparable or smaller than the desorption equilibrium constant, K_d. The shape and position of the breakthrough curve becomes constant when $c_0 \gg K_d$.

The inlet protein concentration effect on protein dimensionless concentration profiles in the adsorbent pore liquid (average), c_{iiAV}/c_0, is shown in Figures 4. As the inlet concentration increases, the average protein concentration in the adsorbent pore-liquid, at the column entrance, reached faster the inlet concentration, (100, 75 and 50 min, respectively). The film mass transfer resistance and dispersion effect can also be observed.

The effect of the inlet protein concentration on the adsorbed phase (average), q_{AVi}/q_m, is shown in Figure 4. A greater degree of column saturation, q_{iAV}/q_m (0.71, 0.80 and 0.85 respectively) is observed in accordance with the Langmuir isotherm, and also a shorter equilibration time is needed (100, 60 and 40 min respectively).

The process parameter of most interest is the bead diameter. In the simulation studies the bead diameter was changed using ± 50% variations of the $d_p = 100$ μm base value. The corresponding curves are shown in Figure 5.

A sharper breakthrough curve, consequently a greater operation capacity, is obtained as the bead diameter decreases (Figure 5). It can also be noted in the figure that this effect is less dramatic as the bead size decreases. As particle diameter decreases the initial adsorption rate increases markedly, since the diffusion time is decreased due to the shorter diffusion path. At the same time the area/volume ratio for a single particle $(3/r_m)$ increases, giving an increased mass transfer area between the surrounding liquid phase and the bead. Both factors contribute to the increase in total adsorption rate.

The bead diameter effect on the profiles c_{iAV}/c_0 is shown in Figure 5. As particle diameter decreases, the film mass transfer resistance and dispersion effects are less marked. At the column entrance, the average protein concentration in the adsorbent pore liquid reached the column inlet concentration in shorter time as particle diameter decreases, (35, 75 and 135 min respectively).

The concentration profiles in the adsorbed phase (Figure 5) show that the degree of column saturation, q_{iAV}/q_m, was reached in shorter time as particle diameter decreases (30, 60 and 120 min respectively), although the particle diameter do not cause an effect on the degree of column saturation value.
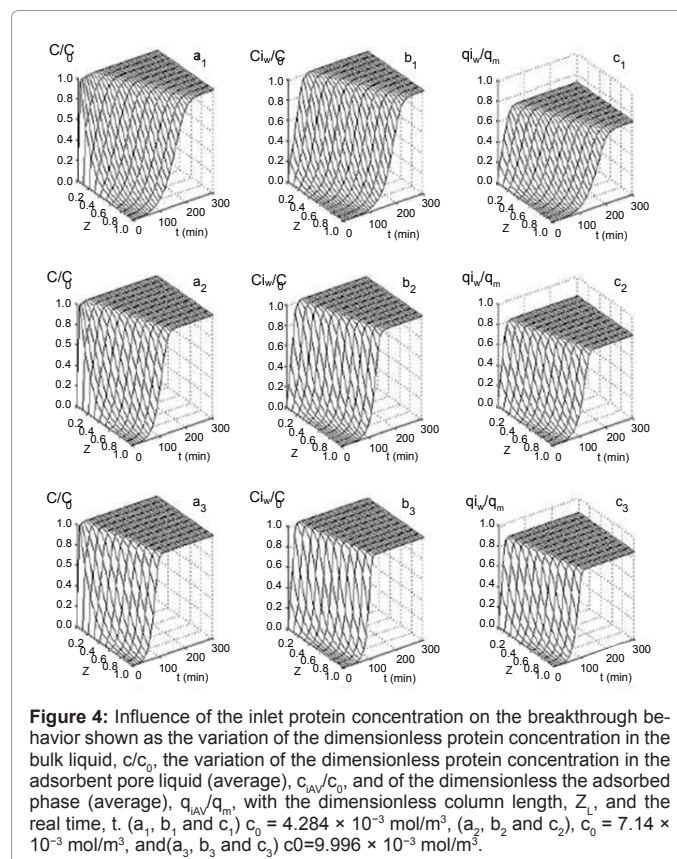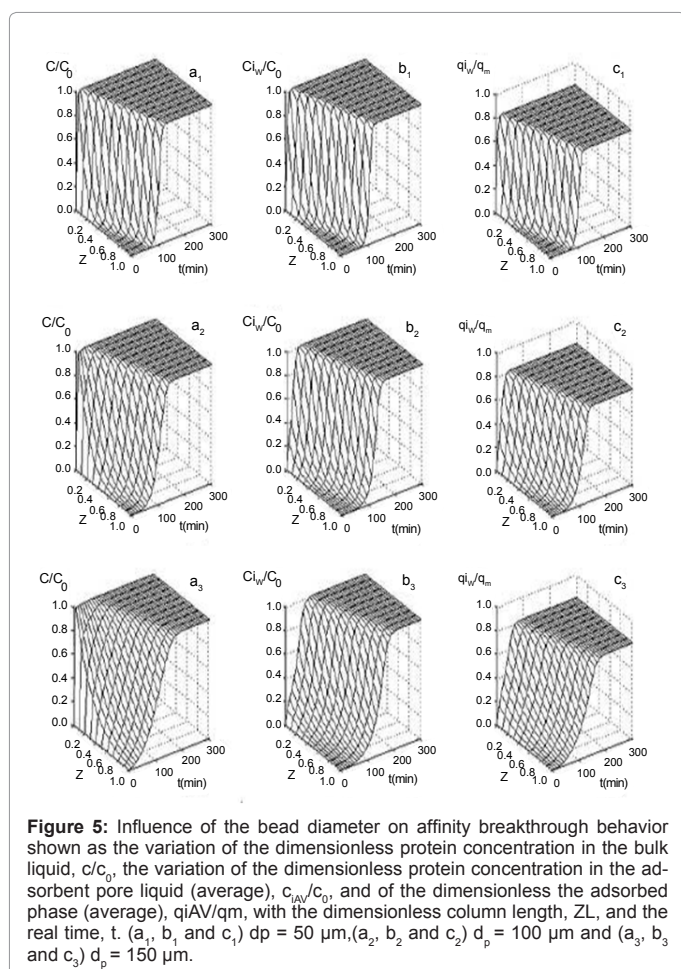

Figure 4: Influence of the inlet protein concentration on the breakthrough behavior shown as the variation of the dimensionless protein concentration in the bulk liquid, c/c_0, the variation of the dimensionless protein concentration in the adsorbent pore liquid (average), c_{iAV}/c_0, and of the dimensionless the adsorbed phase (average), q_{iAV}/q_m, with the dimensionless column length, Z_L, and the real time, t. (a_1, b_1 and c_1) $c_0 = 4.284 \times 10^{-3}$ mol/m³, (a_2, b_2 and c_2), $c_0 = 7.14 \times 10^{-3}$ mol/m³, and(a_3, b_3 and c_3) c0 = 9.996 × 10^{-3} mol/m³.

Figure 5: Influence of the bead diameter on affinity breakthrough behavior shown as the variation of the dimensionless protein concentration in the bulk liquid, c/c_0, the variation of the dimensionless protein concentration in the adsorbent pore liquid (average), c_{iAV}/c_0, and of the dimensionless the adsorbed phase (average), q_{iAV}/q_m, with the dimensionless column length, Z_L, and the real time, t. (a_1, b_1 and c_1) $d_p = 50$ μm, (a_2, b_2 and c_2) $d_p = 100$ μm and (a_3, b_3 and c_3) $d_p = 150$ μm.

Conclusions

The performance of frontal affinity chromatography of lysozyme to Cibacron Blue Sepharose CL-6B Sepharose was successfully described with a three-resistances and column dispersed flow model. Programming the model solution was quite simple using MOL in MATLAB platform. Additionally, parametric studies performed helped to gain qualitative information and to show the influence of both operation and system parameters on the affinity process. An early and sharper breakthrough curve and therefore a greater operating throughput of the affinity process was obtained as the column inlet concentrations were increased. In the bead-size parametric study, a sharper breakthrough curve and consequently a greater operating throughput was attained as the bead diameter decreases. This effect was less dramatic as the bead size decreases. The dynamic responses obtained are in concordance with theoretical predictions and show that the transport model can be used as a framework to provide a general description of almost all practical systems, when the appropriate basic experimental parameters and numerical solution are used, in order to obtain good simulation results. The MATLAB solution of the transport model permitted an accurate prediction of the frontal affinity performance and a better understanding of the fundamental mechanisms responsible for the separation. The influence of the adsorption properties of the protein from other components present in more complex mixtures should enable the work described here with a model system to be extended to more practical situations.

References

1. Persson P, Kempe H, Zacchi G, Nilsson B (2004) A methodology for estimation of mass transfer parameters in a detailed chromatography model based on frontal experiments. Chem Eng Res Des 82: 517-526.

2. Boi C, Dimartino S, Sarti GC (2007) Modelling and simulation of affinity membrane adsorption. J Chromatogr A 1162: 24-33.

3. Karlsson D, Jakobsson N, Axelsson A, Nilsson B (2004) Model-based optimization of a preparative ion-exchange step for antibody purification. J Chromatogr A 1055: 29-39.

4. Kempe H, Persson P, Axelsson A, Nilsson B, Zacchi G (2006) Determination of diffusion coefficients of proteins in stationary phases by frontal chromatography. Biotechnol Bioeng 93: 656-664.

5. Montesinos RM, Tejeda-Mansir A, Guzman R, Ortega J, Schiesser WE (2005) Analysis and simulation of frontal affinity chromatography of proteins. Sep Purif Technol 42: 75-84.

6. Liapis AI, Unger KK (1994) Highly Selective Separations in Biotechnology. (G. Street edn), Chapman and Hall, London.

7. Lee HS, Matthews CJ, Braddock RD, Sander GC, Gandola F (2004) A MATLAB method of lines template for transport equations. Environ Modell Softw 19: 603-614.

8. Chase HA (1984) Prediction of the performance of preparative affinity chromatography. J Chromatogr 297: 179-202.

9. Thomas HC (1944) Heterogeneous Ion Exchange in a Flowing System. J Am Chem Soc 66: 1664-1666.

10. Horstmann BJ, Chase HA (1989) Modelling the affinity adsorption of immunoglobulin *G* to protein *A* immobilised to agarose matrices. Chem Eng Res Des 67: 243-254.

11. Arve BH, Liapis AI (1987) Modeling and analysis of biospecific adsorption in a finite bath. AIChE Journal 33: 179-193.

12. Berninger JA, Whitley RD, Zhang X, Wang NHL (1991) A versatile model for simulation of reaction and nonequilibrium dynamics in multicomponent fixed-bed adsorption processes. Comput Chem Eng 15: 749-768.

13. Kempe H, Axelsson A, Nilsson B, Zacchi G (1999) Simulation of chromatographic processes applied to separation of Proteins. J Chromatogr A 846: 1-12.

14. Ruthven DM (1984) Principles of Adsorption and Adsorption Processes. New York: John Wiley and Sons.

15. Wouwer AV, Saucez P, Schiesser WE (2004) Simulation of Distributed Parameter Systems Using a Matlab-Based Method of Lines Toolbox: Chemical Engineering Applications. Ind Eng Chem Res 43: 3469-3477.

16. Schiesser WE, Griffiths GW (2009) A Compendium of Partial Differential Equation Models: Method of Lines Analysis with Matlab. New York : Cambridge University Press.

17. Shampine LF, Reichelt MW (1997) The MATLAB ODE suite. 1-33.

18. Arnold FH, Blanch HW, Wilke CR (1985) Analysis of affinity separations: I: Predicting the performance of affinity adsorbers. Chem Eng J 30: B9-B23.

19. Danckwerts PV (1953) Continuous flow systems: Distribution of residence times. Chem Eng Sci 2: 1-13.

20. Ashino R, Nagase M, Vaillancourt R (2000) Behind and beyond the MATLAB ODE Suite. Comput Math Appl 40: 491-512.

21. Schiesser WE, Silebi CA (1997) Computational Transport Phenomena: Numerical Methods for the Solution of Transport Problems. New York: Cambridge University Press.

22. Hiester NK, Vermeulen T (1952) Saturation performance of ion-exchange and adsorption columns. Chem Eng Prog 48: 505-516.

23. Foo SC, Rice RG (1975) On the prediction of ultimate separation in parametric pumps. AIChE Journal 21: 1149-1158.